



Structure–activity relationship studies of naphthol AS-E and its derivatives as anticancer agents by inhibiting CREB-mediated gene transcription

Bingbing X. Li ^{a,b}, Kinrin Yamanaka ^{a,b}, Xiangshu Xiao ^{a,b,c,*}

^a Program in Chemical Biology, Oregon Health & Science University, 3181 SW Sam Jackson Park Rd, Portland, OR, USA

^b Department of Physiology and Pharmacology, Oregon Health & Science University, 3181 SW Sam Jackson Park Rd, Portland, OR, USA

^c Knight Cancer Institute, Oregon Health & Science University, 3181 SW Sam Jackson Park Rd, Portland, OR, USA

ARTICLE INFO

Article history:

Received 23 August 2012

Revised 18 September 2012

Accepted 27 September 2012

Available online 4 October 2012

Keywords:

CREB
CBP
Cancer
Naphthol AS-E
Inhibitor
Transcription

ABSTRACT

CREB (cyclic AMP-response element binding protein) is a downstream transcription factor of a multitude of signaling pathways emanating from receptor tyrosine kinases or G-protein coupled receptors. CREB is not activated until it is phosphorylated at Ser133 and its subsequent binding to CREB-binding protein (CBP) through kinase-inducible domain (KID) in CREB and KID-interacting (KIX) domain in CBP. Tumor tissues from various organs present higher level of expression and activation of CREB. Thus CREB has been proposed as a promising cancer drug target. We previously described naphthol AS-E (**1a**) as a small molecule inhibitor of CREB-mediated gene transcription in living cells. Here we report the structure–activity relationship (SAR) studies of **1a** by modifying the appendant phenyl ring. All the compounds were evaluated for *in vitro* inhibition of KIX–KID interaction, cellular inhibition of CREB-mediated gene transcription and inhibition of proliferation of four cancer cell lines (A549, MCF-7, MDA-MB-231 and MDA-MB-468). SAR indicated that a small and electron-withdrawing group was preferred at the *para*-position for KIX–KID interaction inhibition. Compound **1a** was selected for further biological characterization and it was found that **1a** down-regulated the expression of endogenous CREB target genes. Expression of a constitutively active CREB mutant, VP16-CREB in MCF-7 cells rendered the cells resistant to **1a**, suggesting that CREB was critical in mediating its anticancer activity. Furthermore, **1a** was not toxic to normal human cells. Collectively, these data support that **1a** represents a structural template for further development into potential cancer therapeutics with a novel mechanism of action.

© 2012 Elsevier Ltd. All rights reserved.

1. Introduction

Cancer is a group of heterogeneous diseases with dysregulation in a multitude of cell signaling pathways, which ultimately alter the gene transcription programs in the cells. Various transcription factors are implicated in these processes and therefore have been

proposed as promising anticancer drug targets.¹ The cyclic-AMP (cAMP)-response element (CRE)² binding protein (CREB) is one of the transcription factors that critically regulate the development and maintenance of tumor cells.^{2,3} CREB is a stimulus-induced transcription factor activated by multiple extracellular signals through phosphorylation.⁴ The transcription activity of CREB depends on its phosphorylation at Ser133 by mitogen- and stress-activated protein serine/threonine kinases, which include protein kinase A (PKA), protein kinase B (PKB/Akt), mitogen-activated protein kinase (MAPK) and 90 kD protein ribosomal S6 kinase (pp90^{RSK}).⁵ The phosphorylated CREB (p-CREB) can then bind the mammalian transcription co-activator, CREB-binding protein (CBP), via the kinase-inducible domain (KID) in CREB and KID-interacting (KIX) domain in CBP.⁶ This CREB–CBP complex then recruits other transcriptional machinery to the gene promoter to initiate CREB-dependent gene transcription.⁴

CREB participates in the regulation of immortalization and transformation of normal cells and is overexpressed/overactivated in many different types of cancers.^{2,7} In human prostate cancers,

Abbreviations: ALL, acute lymphoid leukemia; AML, acute myeloid leukemia; bcl-2, B-cell lymphoma-2; CBP, CREB-binding protein; CRE, cAMP-response element; CREB, CRE-binding protein; ER, estrogen receptor; FACS, fluorescence-activated cell sorting; FBS, fetal bovine serum; GAPDH, glyceraldehyde-3-phosphate dehydrogenase; HER2, human epidermal growth factor receptor 2; HFF, human foreskin fibroblast; HMEC, human mammary epithelial cells; HPRT, hypoxanthine phosphoribosyltransferase; KID, kinase-inducible domain; KIX, KID-interacting; MAPK, mitogen-activated protein kinase; NSCLC, non-small-cell lung cancer; PARP, poly (ADP-ribose) polymerase; p-CREB, phosphorylated CREB; PKA, protein kinase A; PKB, protein kinase B; PI, propidium iodide; pp90^{RSK}, 90 kD protein ribosomal S6 kinase; PR, progesterone receptor; qRT-PCR, quantitative reverse transcriptase polymerase chain reaction; VEGF, vascular endothelial growth factor; VP16, viral protein 16.

* Corresponding author. Tel.: +1 503 494 4748; fax: +1 503 494 4352.

E-mail address: xiaoxi@ohsu.edu (X. Xiao).

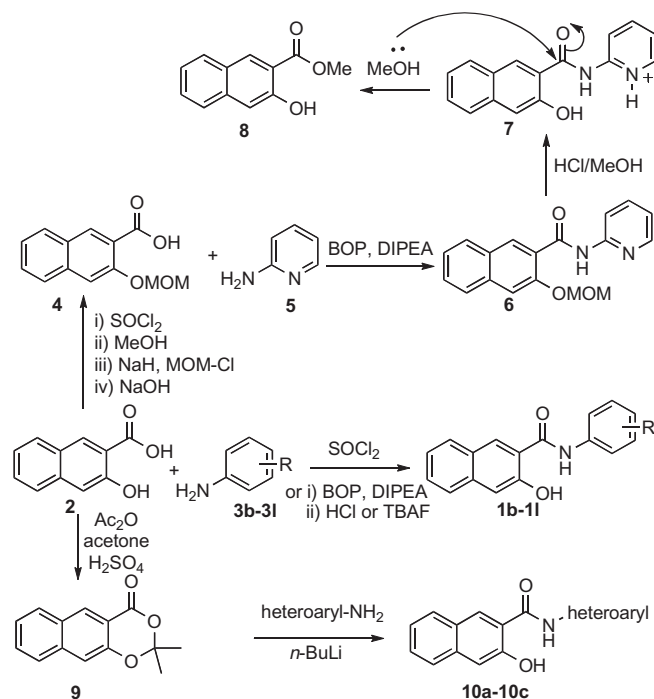
immunohistochemical analysis of primary and bone metastatic prostate cancer tissues from patients demonstrated that normal or benign prostate glands showed no detectable *p*-CREB.⁸ On the other hand, positive *p*-CREB staining was consistently detected in poorly-differentiated cancers and bone metastatic tissue specimens.⁸ This positive correlation between the level of *p*-CREB and the extent of tumor differentiation and metastasis suggests that CREB may be involved in tumor progression and metastasis. Overexpression of CREB was also seen in the cancer tissues from breast cancer patients,⁹ non-small-cell lung cancer (NSCLC) patients,¹⁰ and the blast cells from patients with acute myeloid leukemia (AML).¹¹ Conversely, the expression of CREB-targeting miR-34b was significantly down-regulated in the bone marrow samples from AML patients.¹² These studies indicate that CREB not only can serve as a potential diagnostic marker for various cancers,¹³ but also can be exploited as a potential cancer therapeutic target.² Indeed, inhibiting CREB's transcription activity using different genetic methods, including RNA interference (RNAi),¹¹ CRE-decoy oligonucleotides,¹⁴ and dominant-negative CREB mutants,^{15,16} has demonstrated anticancer activity in different models. To translate these discoveries into potential cancer therapeutics would require identification of appropriate small molecule inhibitors of CREB-mediated gene transcription.

Recently, we described that naphthol AS-E (**1a**, Chart 1) binds KIX and is a cell-permeable small molecule inhibitor of KIX–KID interaction,¹⁷ an essential interaction for CREB-dependent gene transcription activation. As a result, compound **1a** is able to inhibit CREB-mediated gene transcription in living cells.¹⁷ However, it remains to be established whether small molecule inhibitors of CREB-mediated gene transcription like **1a** have any utility as anti-cancer agents. Herein we report the structure–activity relationships of **1a** and present data to show that **1a** is selectively toxic to cancer cells and it displays CREB-dependent anticancer activity.

2. Results and discussion

2.1. Chemistry

In order to delineate the structural elements in **1a** critical for inhibition of KIX–KID interaction, 3-hydroxy-2-naphthamides derived from differentially substituted anilines or heteroaromatic amines were designed. The synthesis of these compounds is presented in Scheme 1. Most of the anilines **3** could directly couple with unprotected acyl chloride derived from acid **2** and SOCl₂ to give final products **1**.¹⁸ Protection of the additional 4-NH₂ or 4-OH group in anilines **3g–3h** with Boc or TBS was required. In these cases, the coupling between protected anilines and acid **2** was carried out by BOP/DIPEA instead of SOCl₂. The protecting groups Boc and TBS were then removed by HCl and TBAF, respectively. When a heteroaryl amine such as **5** (Scheme 1) was used for direct coupling with acyl chloride derived from **2**, it was found that the nucleophilicity of the amine was insufficient to compete with the free hydroxyl group in **2** and therefore no desired amide product could be isolated. To circumvent this issue, the MOM ether **4** was prepared by a 4-step sequence involving esterification, MOM protection and saponification. Coupling between **4** and **5** in the presence of BOP reagent gave amide **6**. However, when compound



Scheme 1. Synthesis of compounds **1** and **10**.

6 was subjected to MOM deprotection under acidic condition (HCl/MeOH), only methyl ester **8** was obtained, which was presumably formed through a protonated intermediate **7**. The acidic lability of amide **6** led us to investigate an alternative route via acetonide **9** (Scheme 1), which was prepared from **2** and acetone/Ac₂O in the presence of catalytic amount of H₂SO₄.¹⁹ Nucleophilic ring opening of **9** with heteroaryl amines provided **10a–10c**. A strong base like *n*-BuLi was necessary for these successful coupling reactions because weaker bases such as DIPEA or DBU did not generate desired products.

2.2. Structure–activity relationships

All the synthesized compounds were evaluated for their activity in inhibiting KIX–KID interaction in vitro using a Renilla luciferase complementation assay we recently developed.¹⁷ The cellular activity of the compounds in inhibiting CREB-mediated gene transcription was investigated by a CREB Renilla luciferase reporter assay in HEK 293T cells.¹⁷ As shown in Table 1, the *para*-chlorine atom in **1a** was important to the inhibition of KIX–KID interaction because *meta*- (**1b**) or *ortho*-substituted (**1c**) analogue displayed decreased inhibition. Because of this requirement of *para*-substitution, the remaining compounds were mainly designed to have different substitutions at this position. In the halogen series, a potency trend of 4-F (**1d**) > 4-Cl (**1a**) > 4-Br (**1e**) > 4-I (**1f**) was observed in inhibiting KIX–KID interaction in vitro, suggesting that increased steric bulkiness and/or decreased electron-withdrawing potential at this position were detrimental to KIX–KID interaction inhibition. To further dissect if both of these two parameters were critical for KIX–KID interaction inhibition, electron-donating but small groups 4-NH₂ (**1g**) and 4-OH (**1h**) were designed to probe electronic effect while electron-withdrawing but relatively bulky 4-CF₃ (**1i**) was designed to probe steric effect. The diminished activity observed for these three compounds (**1g–1i**) indicated that small and electron-withdrawing groups were favorable at this position to preserve KIX–KID interaction inhibition. The complete loss of inhibition of KIX–KID interaction by **1j** (4-OCH₃) further

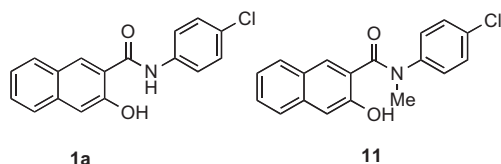


Chart 1. Chemical structures of **1a** and N-methylated compound **11**.

Table 1
Biological activities of **1** and **10**

Compd	R or heteroaryl	IC ₅₀ (μM) ^a		GI ₅₀ (μM) ^b				Average ^g
		KIX–KID inhibition ^c	CREB inhibition ^d	A549	MCF-7	231 ^e	468 ^f	
1a	4-Cl	2.90 ± 0.81	2.29 ± 0.31	2.90 ± 0.33	2.81 ± 0.35	2.35 ± 0.60	1.46 ± 0.30	2.38
1b	3-Cl	>50	2.70 ± 1.34	3.68 ± 0.37	2.43 ± 0.62	4.91 ± 0.83	2.58 ± 0.88	3.40
1c	2-Cl	5.43 ± 0.80	5.72 ± 1.80	4.83 ± 0.57	2.27 ± 0.59	17.15 ± 5.69	6.65	7.73
1d	4-F	1.73 ± 0.22	4.86 ± 2.17	6.78 ± 1.32	4.16 ± 3.17	11.42 ± 0.86	2.78 ± 0.90	6.29
1e	4-Br	9.59 ± 1.35	3.45 ± 0.07	3.98 ± 0.65	1.83 ± 0.70	9.93 ± 2.56	6.61 ± 3.62	5.59
1f	4-I	34.5 ± 3.96	4.98 ± 1.73	5.51 ± 0.83	9.76 ± 6.31	7.87 ± 3.03	2.94 ± 0.51	6.52
1g	4-NH ₂	25.41 ± 13.28	>50	51.56 ± 11.94	27.97 ± 4.63	>100	57.06 ± 8.47	59.15
1h	4-OH	28.23 ± 17.07	40.53 ± 13.40	28.14	9.52 ± 5.99	>100	65.33 ± 38.27	50.75
1i	4-CF ₃	>50	6.75 ± 4.06	4.15 ± 0.50	3.62 ± 2.56	64.21 ± 50.62	63.32 ± 51.88	33.83
1j	4-OCH ₃	>50	>50	85.65 ± 8.74	6.55 ± 2.28	75.46 ± 34.70	79.26 ± 29.34	61.73
1k	3,4-F	2.39 ± 0.81	3.73 ± 0.86	3.57 ± 0.23	2.09 ± 0.82	11.55 ± 12.93	4.19 ± 3.65	5.35
1l	3-Cl-4-F	5.13 ± 3.30	2.29 ± 0.22	3.65 ± 0.36	6.86 ± 5.65	2.20 ± 0.46	0.85 ± 0.047	3.39
10a	2-Pyridine	1.69 ± 0.071	>50	75.84 ± 23.14	6.25 ± 5.89	44.17 ± 3.88	5.69 ± 4.04	32.99
10b	4-Pyridine	16.32 ± 9.58	20.72 ± 6.05	25.03 ± 10.69	15.76 ± 5.29	35.54 ± 6.28	63.44 ± 51.71	34.94
10c	Pyridazine	20.34 ± 7.19	>50	33.24 ± 2.88	17.92 ± 13.77	>100	37.63 ± 3.29	47.20

^a The IC₅₀ is presented as mean ± SD of at least two independent experiments or >50 in the cases where IC₅₀ did not reach at the highest tested concentration (50 μM).

^b GI₅₀ is the concentration required to inhibit the cancer cell growth by 50% as evaluated by the MTT assay. The compounds were incubated with cells for 72 h. The GI₅₀ is presented as mean ± SD of at least two independent experiments or >100 in the cases where GI₅₀ did not reach at the highest tested concentration (100 μM). When SD was not presented, only one experiment was performed in duplicates.

^c KIX–KID interaction inhibition was evaluated by an in vitro Renilla luciferase complementation assay.

^d CREB inhibition refers to inhibition of CREB-mediated gene transcription in HEK 293T cells using a CREB reporter assay.

^e MDA-MB-231 cell line.

^f MDA-MB-468 cell line.

^g Average of the mean GI₅₀ of A549, MCF-7, MDA-MB-231 and MDA-MB-468.

supported this conclusion. Introducing additional substitution at the 3-position of the most potent compound (**1d**) resulted in **1k** and **1l**, both of which displayed slightly reduced activity compared to **1d**. Three heteroaryl amides (**10a–10c**) were also designed to further interrogate the electronic effect. While 2-pyridine-substituted analogue **10a** exhibited good activity, the 4-pyridine-(**10b**) and pyridazine-(**10c**) substituted analogues presented significantly reduced activity. Overall, these results suggest the binding site in KIX for the 4-chlorophenyl ring in **1a** is relatively small and of moderate hydrophobicity.

In a cell-based CREB Renilla luciferase reporter assay, compound **1a** inhibited CREB-mediated gene transcription with an IC₅₀ of 2.29 μM (Table 1).¹⁷ Consistent with its decreased in vitro potency in inhibiting KIX–KID interaction, the *ortho*-substituted **1c** also showed diminished activity in inhibiting CREB's activity in HEK 293T cells. In the case of **1b**, which did not inhibit KIX–KID interaction in vitro, it still presented good cellular CREB transcription inhibition activity. A similar difference was also observed with **1i**. This apparent discrepancy would suggest that the cellular activity seen with **1b** and **1i** was independent of KIX–KID interaction. In the halogen series (**1a**, **1d–1f**), the potency trend was not as clear as their in vitro KIX–KID interaction potency. For example, **1d** was most potent in inhibiting KIX–KID interaction in vitro, but it was not the most potent compound in cellular inhibition of CREB's activity. Analogues with electron-donating groups (**1g**, **1h**, **1j**) at the *para*-position generally displayed poor cellular activity, which is consistent with their weak in vitro potency. The heteroaryl amides **10a–10c** were also poor inhibitors of CREB-mediated gene transcription in HEK 293T cells even though **10a** was a potent KIX–KID interaction inhibitor. This might be resulting from altered cell permeability²⁰ of the substituted pyridine, whose relative cell permeability is very sensitive to substitution.²¹

Given the potentially important role of CREB signaling in the maintenance of cancer phenotype,² the synthesized compounds were evaluated for their potential in inhibiting cancer cell growth using an MTT assay.²² A small panel of cancer cell lines including A549 (non-small cell lung cancer), MCF-7 (breast cancer, positive for estrogen receptor (ER⁺)), triple negative breast cancer cell lines

MDA-MB-231 and MDA-MB-468, which do not express ER, PR (progesterone receptor) or HER2 (human epidermal growth factor receptor 2), was used (Table 1). The lead compound **1a** exhibited low μM activity in inhibiting the proliferation of all these cancer cells, which is consistent with its cellular CREB inhibition potency. In fact, this compound inhibited the growth of most of the cancer cells in the NCI-60 cancer cell panel (Fig. S1). In general, there was a good correlation between the cellular inhibition of CREB's activity and growth inhibition of cancer cells (Table 1). When the average GI₅₀ value, which is the average of the mean GI₅₀ of A549, MCF-7, MDA-MB-231 and MDA-MB-468, was plotted against the cellular IC₅₀ of CREB inhibition, there was an excellent correlation ($r^2 = 0.817$, $P < 0.0001$, Fig. 1). Compounds **1g**, **1h**, **1j** and **10a** did not show appreciable inhibition of CREB-mediated gene transcription, however, they all had moderate growth inhibitory activity in MCF-7 cells, but not in other cancer cell lines tested. These results suggest that these compounds may inhibit the growth of MCF-7 cells through a non-CREB-related mechanism. Among the analogues prepared in Table 1, compound **1a** represented a good profile of inhibition of KIX–KID interaction in vitro, cellular

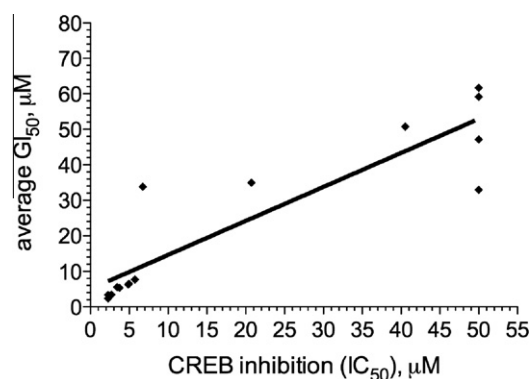


Figure 1. Correlation between inhibition of CREB-mediated gene transcription in HEK 293T cells and average growth inhibition of cancer cells including A549, MCF-7, MDA-MB-231 and MDA-MB-468 by compounds **1** and **10**.

inhibition of CREB-mediated gene transcription and inhibition of cancer cell growth. Therefore, **1a** was selected for further biological characterization as a lead for novel anti-cancer agents.

2.3. Biology

2.3.1. **1a** down-regulated CREB target gene expression

CREB is a transcription factor and its biological functions are primarily mediated by transcription activation of its target genes. Although the exact mechanisms by which CREB contributes to the cancer development are not well understood,² it is hypothesized that some of the CREB target genes critical for anti-apoptosis and/or proliferation are up-regulated in cancer cells.² Therefore, we investigated whether **1a** could down-regulate CREB target genes in A549 cells. Among the many possible cellular CREB targets,²³ we first examined the expression of anti-apoptotic protein Bcl-2,^{24,25} which is often overexpressed in cancer cells and associated with resistance to cancer chemotherapies.^{26,27} As presented in Figure 2A, the expression level of Bcl-2 protein was decreased with increasing concentrations of **1a** in A549 cells. The expression of vascular endothelial growth factor (VEGF), another CREB target,⁸ was also down-regulated in **1a**-treated cells (Fig. 2D). On the other hand, the expression of p21, whose expression is primarily regulated by p53²⁸ and not by CREB,²⁹ was unchanged in all the concentrations tested. Consistent with this result, we found that p53-mediated gene transcription was not inhibited by **1a** using a transcription reporter assay (Fig. S2). These results demonstrated that **1a** did not inhibit cellular gene expression non-specifically.

To probe whether the reduction of Bcl-2 and VEGF expression was due to a decrease of their respective mRNA level upon treatment with **1a** as would be expected given its mechanism of action, quantitative reverse transcriptase polymerase chain reaction (qRT-PCR) was employed to investigate the relative level of transcripts. Upon treatment of A549 cells with **1a** for 4 h, the transcript levels of *bcl-2* and *VEGF* were decreased (Fig. 2B and S3). Consistent with the Western blot results (Fig. 2A), the transcript level of *p21* was essentially unchanged upon treatment with **1a** (Fig. 2C), further arguing that the reduction of *bcl-2* and *VEGF* was not non-specific.

2.3.2. **1a** induced apoptosis in A549 cells

Because **1a** down-regulated the expression of anti-apoptotic protein Bcl-2, we investigated if programmed cell death or apoptosis was induced upon treatment with **1a** in A549 cells. Fluorescence-activated cell sorting (FACS) analysis was employed to analyze **1a**-treated A549 cells after being stained with annexin-V and propidium iodide (PI) (Fig. 3). In this two-dye binding assay, annexin-V would bind phosphatidylserine exposed on the dying apoptotic cell surface while PI would only stain dead cells whose plasma-membrane integrity was compromised.^{30,31} There was a dose-dependent increase in the population of annexin⁺/PI⁻ cells, indicative of cells undergoing apoptosis. Up to 19.4% of the cells treated with 10 μ M of **1a** were undergoing apoptosis, compared to only 3.9% of the vehicle-treated cells (Fig. 3). Consistent with the conclusion of activation of apoptosis, cleavage of poly (ADP-ribose) polymerase (PARP),³² another marker of apoptosis, was observed in A549 cells treated with **1a** (Fig. 2A). Collectively, these

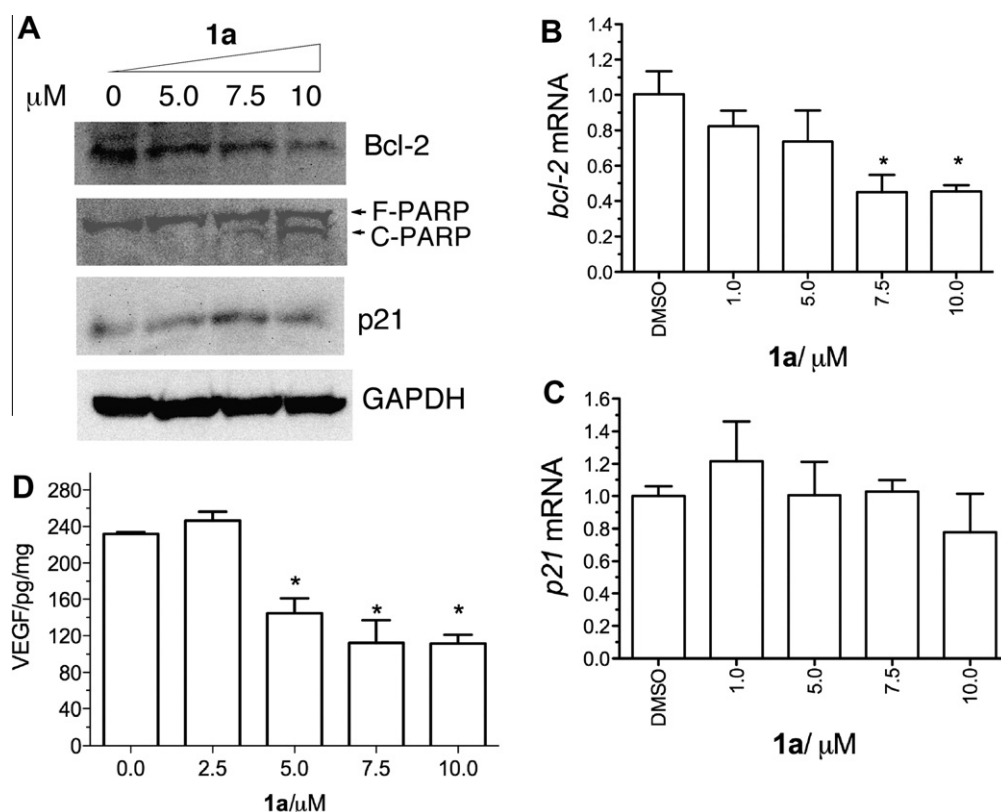


Figure 2. Compound **1a** inhibited CREB targets Bcl-2 and VEGF expression. (A) Exponentially growing A549 cells were treated with different concentrations of **1a** for 48 h. The cells were then harvested and lysed in Nonidet P-40 lysis buffer. Then the proteins were separated on a 10% SDS-PAGE gel. The indicated proteins were detected by their corresponding antibodies after being transferred to a PVDF membrane. GAPDH was used as a loading control. (B and C) The mRNA level of *bcl-2* (B, * $P < 0.05$ by one-way ANOVA), but not *p21* (C, $P = 0.34$), was decreased in A549 cells upon treatment with **1a**. A549 cells were treated with **1a** at indicated concentrations in duplicate for 4 h. Total RNA was isolated from the treated cells and converted into cDNA using random hexamers as primers. The relative amount of the transcript was analyzed by qPCR with SYBR[®] Green and normalized to *HPRT*. (D) A549 cells in a 96-well plate were treated with indicated concentrations of **1a** in duplicate for 24 h. Then VEGF concentration in the culture media was determined by a VEGF ELISA assay. The concentration of VEGF was normalized to the protein concentration in the culture media. * $P < 0.05$ by one-way ANOVA.

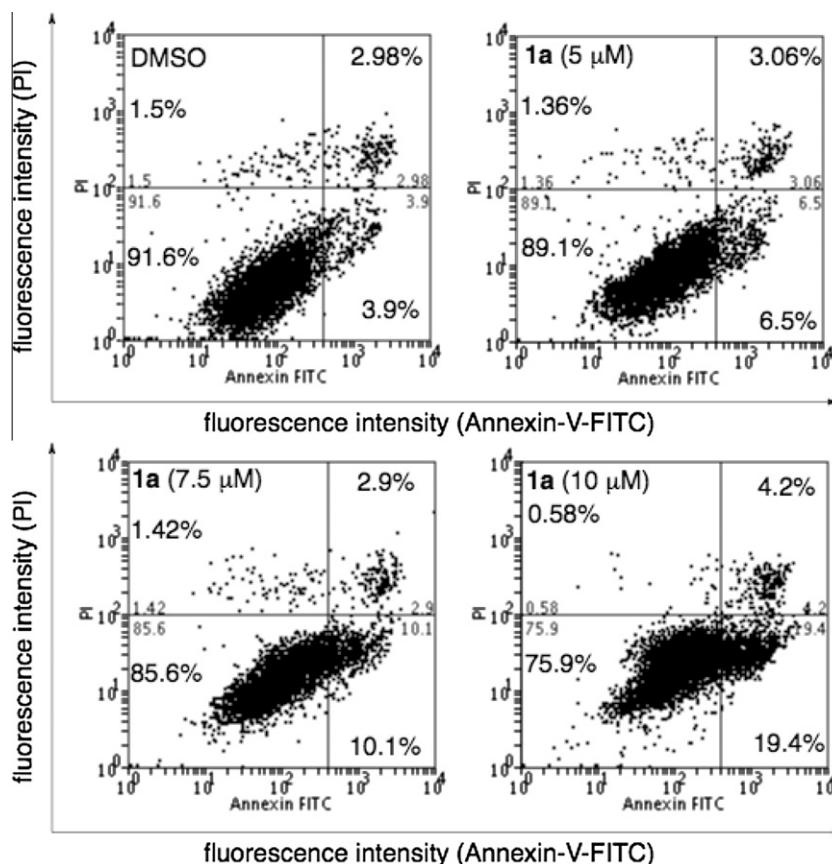


Figure 3. Compound **1a** induced apoptosis in A549 cells. Exponentially growing A549 cells were treated with **1a** at different concentrations for 48 h. The cells were harvested, washed with cold PBS, and then stained with fluorescein-labeled annexin V (annexin-V-FITC) and propidium iodide (PI). The cells were then analyzed by flow cytometry with FACS Calibur. The data were analyzed by Weasel v2.5 (the numbers in each quadrant showed the percentage of cells in the corresponding quadrants).

data demonstrated that **1a** activated an apoptotic cell death program in A549 cells.

2.3.3. **1a**-mediated cancer cell growth inhibition was dependent on CREB

Cancer cells can undergo growth inhibition and/or apoptosis through a myriad of mechanisms. And a major challenge for any given targeted cancer therapeutic is to verify that the observed cancer cell growth inhibition is a result of on-target effect. To investigate if inhibition of CREB's activity by **1a** was the mechanism through which it inhibited proliferation of cancer cells, a constitutively active CREB mutant, VP16-CREB¹⁷ was ectopically expressed in the cells. Unlike endogenous wild-type CREB whose activity is dependent on phosphorylation, the transcription activity of VP16-CREB is determined by the potent activation domain VP16 and is independent of phosphorylation.³³ We previously showed that **1a** did not inhibit VP16-CREB-mediated gene transcription.¹⁷ It was hypothesized that cells with VP16-CREB would be more resistant to **1a** if CREB-mediated gene transcription were critical to its activities in cancer cells. Therefore, VP16-CREB was stably expressed in breast cancer MCF-7 cells (Fig. 4A). Compared to parental MCF-7 cells, the cells expressing VP16-CREB were more resistant to the treatment of **1a** (Fig. 4B). However, these cells were not completely resistant to **1a**, which was very likely due to the low expression level of VP16-CREB. As a consequence, the endogenous wild-type CREB still played a role in regulating proliferation of these cells. In fact, the expression level of VP16-CREB was less than 1% of endogenous CREB (Fig. S4). Higher expression clones could not be identified presumably because these clones died during the selection process. This phenomenon is similar to other

oncogenes such as c-Myc, which also induces apoptosis when highly expressed.³⁴ However, the minute amount of VP16-CREB in the cells was required for this partial resistance because the sensitivity to **1a** was restored if the expression of VP16-CREB was lost from the cells after they were passaged in non-selecting media (data not shown). In any case, the *N*-methylated compound **11** (Chart 1), which did not inhibit CREB's activity or KIX-KID interaction,¹⁷ was equally effective in both of these cells (Fig. 4C). Collectively, the differential sensitivity seen with compound **1a**, but not compound **11**, indicated the antiproliferative activity of **1a** in MCF-7 cells was at least partially through its inhibition of KIX-KID interaction and CREB-mediated gene transcription.

2.3.4. **1a** was not toxic to normal human cells

CREB is a pleiotropic factor involved in many different cellular processes.^{4,35} Perhaps due to the concerns of potential toxicity effect in normal cells, CREB has not been pharmacologically targeted to develop cancer therapeutics.² Previous genetic studies with hypomorphic CREB mutant showed, however, that mice tolerated well with reduced CREB protein.³⁶ With **1a** as a pharmacological tool, we then asked if pharmacological inhibition of CREB-mediated gene transcription would result in massive undesired side effects in normal cells. To this end, proliferating normal human mammary epithelial cells (HMEC) were treated with increasing concentrations of **1a**. Then the number of live cells was counted after 48-h incubation. In contrast to the cancer cells (Table 1), the results shown in Figure 4D demonstrated that **1a** presented little or no toxicity to these normal cells under the concentrations tested (10 μ M and lower). Although a minor decrease of the number of viable cells was observed at higher concentrations, they

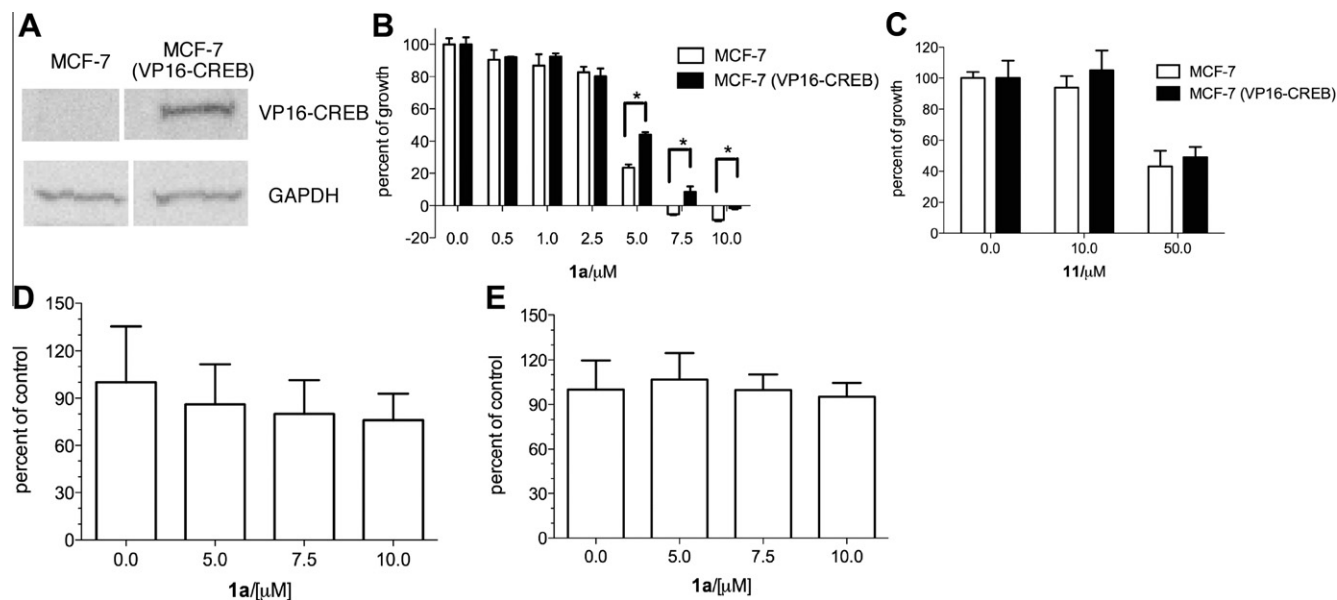


Figure 4. Compound **1a** inhibited MCF-7 cell proliferation through a CREB-dependent mechanism. (A) The cell lysates from MCF-7 cells or MCF-7 cells stably expressing VP16-CREB were separated on a 4–20% SDS-PAGE gel and transferred to a PVDF membrane. The membrane was probed with anti-FLAG (M2) followed by anti-GAPDH. (B and C) Compared to parental MCF-7 cells, MCF-7 cells expressing VP16-CREB were more resistant to **1a** (B), but not control compound **11** (C). The cells were treated with compounds at indicated concentration in triplicate for 48 h. Then the number of live cells was quantified by MTT reagent. * $P < 0.05$ by student's *t*-test. **1a** displayed little or no toxicity to normal HMEC (D) or HFF (E) cells. Cells were treated with increasing concentrations of **1a** in triplicate for 48 h. Then the number of live cells was counted by trypan blue exclusion assay. The differences in HMEC were statistically insignificant ($P = 0.28$ by one-way ANOVA).

were not statistically significant (one-way ANOVA analysis, $P = 0.28$). Using human foreskin fibroblast (HFF) cells as another normal cell type, we did not observe significant toxicity either (Fig. 4E). These results suggest that normal cells are not heavily dependent on CREB for their survival and proliferation. Alternatively, these results could be explained that the residual CREB activity after **1a** treatment was sufficient for the normal cells to maintain their homeostasis, but detrimental to the cancer cells.² This selective toxicity suggests that the transformed cancer cells may be addicted to CREB-mediated gene transcription for survival. This notion is also supported from CREB expression studies in clinical patient samples with acute lymphoid leukemia (ALL), where CREB expression is elevated at diagnosis and decreased to an undetectable level at remission, but then regained at relapse.¹³

3. Conclusion

A series of analogues of **1a** with different substitutions at the appendant phenyl ring was designed and synthesized to interrogate the structural requirements for its activity in inhibiting KIX–KID interaction and CREB-mediated gene transcription. Structure–activity relationship studies indicated that small and electron-withdrawing substituents at the *para*-position were preferred for inhibiting KIX–KID interaction. Given the critical roles played by CREB in cancer cells, these compounds were also evaluated for their activity in inhibiting cancer cell growth. The overall cancer cell growth inhibitory activity was in good correlation with cellular inhibition of CREB-mediated gene transcription in HEK 293T cells. Detailed biological studies with **1a** showed that it induced apoptosis and down-regulated the expression of endogenous CREB target genes. The growth inhibition of cancer cells induced by **1a** was dependent on CREB's activity. Furthermore, we showed that **1a** was not toxic to normal human cells. The selective cytotoxicity suggests that CREB is a viable cancer drug target and **1a** represents a structure for further development into potential cancer therapeutics with a novel mechanism of action.

4. Experimental section

4.1. Chemistry

General information: The solvents used for each reaction were purified from the Glass Contout solvent purification system. Melting points were determined in capillary tubes using Mel-Temp and were uncorrected. All ^1H and ^{13}C NMR spectra were obtained in Bruker Avance 400 MHz spectrometer using either CDCl_3 or $\text{DMSO}-d_6$ or a mixture of these as solvent and the chemical shifts of the residual CHCl_3 (δ 7.24) or DMSO (δ 2.50) were taken as reference. The following abbreviations were used to describe the splitting pattern of individual peaks if applicable: s = singlet, br s = broad singlet, d = doublet, t = triplet, q = quartet, m = multiplet. The coupling constants (*J*) were reported in Hertz (Hz). Silica gel flash chromatography was performed using 230–400 mesh silica gel (EMD, Philadelphia, PA). The mass spectra were obtained from an LTQ Orbitrap Discovery mass spectrometer (Thermo Scientific, West Palm Beach, FL) with electrospray operated either in positive or negative mode. All final compounds for biological evaluations were confirmed to be of >95% purity based on HPLC (Waters, Milford, MA) analysis using an XBridge C18 column (4.6×150 mm) and detected at 254 nm. The mobile phases for HPLC are water and acetonitrile, both of which contained 0.1% TFA.

General procedure A for synthesis of naphthamides by SOCl_2 : Thionyl chloride (0.5 mL) was added to acid **2** (188 mg, 1 mmol) at room temperature. The resulting mixture was then heated under reflux for 1 h. Excess thionyl chloride was removed under reduced pressure and the residue was dissolved with THF (3 mL). An aniline (1.5 mmol) was then added to this solution and the mixture was heated under reflux for another hour. The reaction mixture was cooled to room temperature and the solvent was removed in vacuo. The residue was resuspended in CH_2Cl_2 (3 mL) and the solid was collected by filtration. The resulting solid was treated with 1 N HCl (3 mL) and stirred at room temperature for 30 min. The product was collected by filtration and washed with H_2O (3 mL) and dichloromethane (3 mL) to yield desired naphthamides.

General procedure B for synthesis of naphthamides through 9. *n*-BuLi (2.5 M in hexanes, 0.2 mmol) was slowly added to a stirred solution of a heteroaryl amine (0.2 mmol) in THF (1 mL) at 0 °C. The reaction mixture was stirred at 0 °C for 30 min, when a solution of **9** (0.1 mmol) in THF (1 mL) was slowly added. The reaction mixture was allowed to warm up to room temperature and stirred at room temperature for 1 h. Saturated aqueous NH₄Cl solution (10 mL) was added to quench the reaction. CH₂Cl₂ (50 mL) was then added to dilute the reaction mixture. The organic layer was separated and washed with H₂O (2 × 5 mL) and brine (2 × 5 mL). The organic solution was dried over Na₂SO₄, filtered and the solvent was removed in vacuo. The residue was triturated with hexanes (3 mL) and the solid was collected by filtration, which was then washed with CH₂Cl₂ (1 mL) to give desired amide.

4.1.1. *N*-(3-Chlorophenyl)-3-hydroxy-2-naphthamide (**1b**)

Amide **1b** was obtained using general procedure A as a light brown solid in 52% yield: mp 242–244 °C (Lit.¹⁸ 258–261 °C). ¹H NMR (400 MHz, DMSO-*d*₆) δ 11.15 (s, 1H), 10.69 (s, 1H), 8.43 (s, 1H), 8.00 (t, *J* = 2.0 Hz, 1H), 7.93 (d, *J* = 8.0 Hz, 1H), 7.77 (d, *J* = 8.0 Hz, 1H), 7.66 (dd, *J* = 8.0, 1.0 Hz, 1H), 7.51 (td, *J* = 6.8, 1.2 Hz), 7.41 (t, *J* = 8.0 Hz, 1H), 7.36 (td, *J* = 7.2, 1.2 Hz, 1H), 7.33 (s, 1H), 7.20 (dd, *J* = 8.0, 2.0 Hz, 1H); ¹³C NMR (100 MHz, DMSO-*d*₆) δ 165.8, 153.4, 140.1, 135.7, 133.1, 130.5, 128.7, 128.1, 126.9, 125.8, 123.8, 123.6, 122.4, 119.7, 118.7, 110.5; HRESI-MS for [C₁₇H₁₂ClNO₂-H]⁻, Calcd 296.0484. Found 296.0480.

4.1.2. *N*-(2-Chlorophenyl)-3-hydroxy-2-naphthamide (**1c**)

Amide **1c** was obtained using general procedure A as a light brown solid in 16% yield: mp 214–216 °C (Lit.³⁷ 225 °C). ¹H NMR (400 MHz, DMSO-*d*₆) δ 11.98 (s, 1H), 11.27 (s, 1H), 8.73 (s, 1H), 8.52 (dd, *J* = 8.0, 1.2 Hz, 1H), 8.00 (d, *J* = 8.0 Hz, 1H), 7.79 (d, *J* = 8.4 Hz, 1H), 7.58 (dd, *J* = 8.0, 1.6 Hz, 1H), 7.54 (t, *J* = 7.2 Hz, 1H), 7.42 (t, *J* = 8.4 Hz, 1H), 7.38 (s, 1H), 7.38 (t, *J* = 9.2 Hz, 1H), 7.20 (t, *J* = 8.0 Hz, 1H); ¹³C NMR (100 MHz, DMSO-*d*₆) δ 163.5, 152.7, 136.0, 135.4, 132.7, 129.4, 129.1, 128.5, 127.9, 127.2, 125.7, 125.2, 124.0, 123.3, 122.6, 120.5, 110.8; HRESI-MS for [C₁₇H₁₂ClNO₂-H]⁻, Calcd 296.0484. Found 296.0481.

4.1.3. *N*-(4-Fluorophenyl)-3-hydroxy-2-naphthamide (**1d**)

Amide **1d** was obtained using general procedure A as an off-white solid in 69% yield: mp 256–258 °C. ¹H NMR (400 MHz, DMSO-*d*₆/CDCl₃ (1:1)) δ 11.45 (s, 1H), 10.62 (s, 1H), 8.58 (s, 1H), 7.84 (d, *J* = 8.0 Hz, 1H), 7.73–7.77 (m, 2H), 7.67 (d, *J* = 8.4 Hz, 1H), 7.46 (t, *J* = 7.2 Hz, 1H), 7.31 (t, *J* = 7.2 Hz, 1H), 7.27 (s, 1H), 7.07–7.12 (m, 2H); ¹³C NMR (100 MHz, DMSO-*d*₆/CDCl₃ (1:1)) δ 165.9, 158.5 (d, ¹*J*_{CF} = 240 Hz), 154.3, 135.9, 134.3, 130.3, 128.5, 127.9, 126.6, 125.5, 123.4, 122.4 (d, ³*J*_{CF} = 8 Hz), 119.7, 114.9 (d, ²*J*_{CF} = 22 Hz), 110.6; HRESI-MS for [C₁₇H₁₂FNO₂-H]⁻, Calcd 280.0779. Found 280.0776.

4.1.4. *N*-(4-Bromophenyl)-3-hydroxy-2-naphthamide (**1e**)

Amide **1e** was obtained using general procedure A as a light brown solid in 29.3% yield: mp 248–250 °C (Lit.³⁷ 248–249 °C). ¹H NMR (400 MHz, DMSO-*d*₆) δ 11.21 (br s, 1H), 10.67 (s, 1H), 8.45 (s, 1H), 7.93 (d, *J* = 8.0 Hz, 1H), 7.75–7.77 (m, 3H), 7.57 (dd, *J* = 7.6, 1.6 Hz, 2H), 7.51 (td, *J* = 8.0, 1.2 Hz, 1H), 7.36 (t, *J* = 8.0 Hz, 1H), 7.33 (s, 1H); ¹³C NMR (100 MHz, DMSO-*d*₆) δ 165.7, 153.5, 138.0, 135.7, 132.0, 131.6, 130.5, 128.7, 128.1, 126.9, 125.8, 123.8, 122.3, 115.7, 110.5; HRESI-MS for [C₁₇H₁₂BrNO₂-H]⁻, Calcd 399.9979. Found 399.9975.

4.1.5. 3-Hydroxy-*N*-(4-iodophenyl)-2-naphthamide (**1f**)

Amide **1f** was obtained using general procedure A as an off-white solid in 74% yield: mp > 190 °C (dec). ¹H NMR (400 MHz, DMSO-*d*₆) δ 11.20 (s, 1H), 10.62 (s, 1H), 8.44 (s, 1H), 7.92 (d,

J = 8.0 Hz, 1H), 7.75 (d, *J* = 8.0 Hz, 1H), 7.72 (d, *J* = 8.8 Hz, 2H), 7.61 (d, *J* = 8.8 Hz, 2H), 7.50 (td, *J* = 8.0, 1.2 Hz, 1H), 7.35 (td, *J* = 8.0, 1.2 Hz, 1H), 7.31 (s, 1H); ¹³C NMR (100 MHz, DMSO-*d*₆) δ 165.6, 153.5, 138.4, 137.4, 135.7, 130.5, 128.7, 128.1, 126.8, 125.8, 123.8, 122.5, 122.2, 110.5, 87.7; HRESI-MS for [C₁₇H₁₂INO₂-H]⁻, Calcd 387.9840. Found 387.9835.

4.1.6. *N*-(4-Aminophenyl)-3-hydroxy-2-naphthamide (**1g**)

DIPEA (92 μL, 0.53 mmol) was added to a stirred solution of acid **2** (100 mg, 0.53 mmol) in CH₂Cl₂ (2 mL) at room temperature. Then BOP (234 mg, 0.53 mmol) was added. After 5 min, commercially available *tert*-butyl(4-aminophenyl)carbamate (132 mg, 0.64 mmol) and another portion of DIPEA (111 μL, 0.64 mmol) were sequentially added to the reaction mixture. The reaction mixture was stirred at room temperature for overnight. CH₂Cl₂ (100 mL) was added to dilute the reaction mixture, which was then washed with 1 N HCl (2 × 10 mL), a saturated aqueous solution of NaHCO₃ (2 × 10 mL) and brine (20 mL). The organic solution was then dried over anhydrous Na₂SO₄ overnight, filtered and concentrated yielding a residue that was subjected to silica gel flash chromatography, eluting with hexanes/EtOAc (4:1) to give a light brown solid (126 mg, 63%): mp 208–210 °C. ¹H NMR (400 MHz, DMSO-*d*₆) δ 11.41 (s, 1H), 10.53 (s, 1H), 9.38 (br s, 1H), 8.52 (s, 1H), 7.92 (d, *J* = 8.0 Hz, 1H), 7.76 (d, *J* = 8.4 Hz, 1H), 7.63 (d, *J* = 8.8 Hz, 2H), 7.51 (t, *J* = 7.6 Hz, 1H), 7.46 (d, *J* = 8.8 Hz, 2H), 7.36 (t, *J* = 7.6 Hz, 1H), 7.32 (s, 1H), 1.48 (s, 9 H); ¹³C NMR (100 MHz, DMSO-*d*₆) δ 165.6, 159.6, 154.1, 152.8, 135.9, 132.7, 130.3, 128.8, 128.2, 126.8, 125.8, 123.8, 121.2, 118.4, 110.6, 79.0, 28.2. An aqueous solution of HCl (4 N, 2 mL, 8 mmol) was added to a stirred solution of Boc-protected amide (38 mg, 0.1 mmol) obtained above in THF (2 mL) at room temperature. The resulting mixture was stirred at room temperature for overnight. THF was removed in vacuo and H₂O was azeotropically removed with benzene. The residue was treated with Et₂O (3 mL) and the precipitate was collected by filtration to give an off-white solid (25 mg, 92%): mp > 260 °C (dec). ¹H NMR (400 MHz, DMSO-*d*₆) δ 11.31 (br s, 1H), 10.73 (s, 1H), 10.00 (br s, 2H), 8.49 (s, 1H), 7.93 (d, *J* = 8.0 Hz, 1H), 7.86 (d, *J* = 8.4 Hz, 2H), 7.76 (d, *J* = 8.4 Hz, 1H), 7.51 (t, *J* = 6.8, 1H), 7.33–7.41 (m, 4H); ¹³C NMR (100 MHz, DMSO-*d*₆) δ 165.7, 153.6, 137.8, 135.7, 130.5, 128.7, 128.1, 126.8, 125.8, 123.8, 123.1, 122.0, 121.4, 110.5; HRESI-MS for [C₁₇H₁₄N₂O₂+H]⁺, Calcd 279.1128. Found 279.1128.

4.1.7. 3-Hydroxy-*N*-(4-hydroxyphenyl)-2-naphthamide (**1h**)

DIPEA (85 μL, 0.49 mmol) was added to a stirred solution of acid **2** (92.1 mg, 0.49 mmol) in CH₂Cl₂ (1.6 mL) at room temperature. Then BOP (217 mg, 0.49 mmol) was added. After 5 min, TBS-protected 4-aminophenol³⁸ (121.5 mg, 0.54 mmol) and another portion of DIPEA (94 μL, 0.54 mmol) were sequentially added to the reaction mixture, which was stirred at room temperature for 1 h. The resulting mixture was diluted with CH₂Cl₂ (70 mL) and washed with 1 N HCl (2 × 10 mL), a saturated aqueous solution of NaHCO₃ (2 × 10 mL) and brine (20 mL). The organic solution was then dried over anhydrous Na₂SO₄ overnight, filtered and concentrated yielding a brown oily liquid. The resulting residue was subjected to silica gel flash chromatography, eluting with hexanes/EtOAc (10:1) to give a brown solid that was further triturated with diethyl ether (2 mL) to yield a light brown solid (12.5 mg, 6.5%): mp 218–220 °C. ¹H NMR (400 MHz, DMSO-*d*₆) δ 11.39 (s, 1H), 10.51 (s, 1H), 8.50 (s, 1H), 7.92 (d, *J* = 9.2 Hz, 1H), 7.76 (d, *J* = 8.0 Hz, 1H), 7.63 (d, *J* = 8.8 Hz, 2H), 7.51 (t, *J* = 7.6 Hz, 1H), 7.36 (t, *J* = 7.6 Hz, 1H), 7.32 (s, 1H), 6.88 (d, *J* = 8.4 Hz, 2H), 0.97 (s, 9 H), 0.20 (s, 6H); ¹³C NMR (100 MHz, DMSO-*d*₆) δ 165.6, 154.0, 151.5, 135.8, 132.2, 130.2, 128.7, 128.1, 126.8, 125.8, 123.7, 122.2, 121.4, 119.9, 110.55, 25.6, 18.0, -4.5. TBAF (1.0 M in THF, 70 μL) was added to a stirred solution of *N*-(4-*tert*-butyldimethylsilyloxyphenyl)-3-hydroxy-2-naphthamide (14.6 mg, 0.037 mmol)

in THF (1 mL) at room temperature under argon. The reaction mixture was stirred at room temperature under argon for 4 h. CH₂Cl₂ (80 mL) was added to dilute the resulting mixture, which was then washed with water (2 × 10 mL) and brine (2 × 10 mL). The organic solution was dried over Na₂SO₄ overnight, filtered, and concentrated. The resulting solid was triturated with CH₂Cl₂ (1 mL) and the solid was collected by filtration and washed with water (1 mL) and CH₂Cl₂ (0.5 mL), yielding a light brown solid (3.8 mg, 36.8%); mp > 240 °C. ¹H NMR (400 MHz, DMSO-*d*₆) δ 11.53 (s, 1H), 10.47 (s, 1H), 9.36 (s, 1H), 8.52 (s, 1H), 8.40 (d, *J* = 7.2 Hz, 1H), 7.75 (d, *J* = 7.6 Hz, 1H), 7.49–7.53 (m, 3H), 7.36 (t, *J* = 6.8 Hz, 1H), 7.30 (s, 1H), 6.78 (dd, *J* = 8.8, 2.0 Hz, 2H); ¹³C NMR (100 MHz, DMSO-*d*₆) δ 165.6, 154.4, 154.2, 135.8, 130.1, 129.8, 128.7, 128.2, 126.9, 125.8, 123.8, 122.6, 120.9, 115.2, 110.6; HRESI-MS for [C₁₇H₁₂NO₃-H]⁻, Calcd 278.0823. Found 278.0819.

4.1.8. 3-Hydroxy-*N*-(4-trifluoromethylphenyl)-2-naphthamide (1i)

Amide **1i** was obtained using general procedure A as a light brown solid in 71% yield: mp 276–278 °C. ¹H NMR (400 MHz, DMSO-*d*₆) δ 11.14 (br s, 1H), 10.85 (s, 1H), 8.42 (s, 1H), 8.00 (d, *J* = 8.4 Hz, 2H), 7.94 (d, *J* = 8.4 Hz, 1H), 7.77 (d, *J* = 7.6 Hz, 1H), 7.75 (d, *J* = 8.0 Hz, 2H), 7.51 (t, *J* = 8.0 Hz, 1H), 7.36 (t, *J* = 7.2 Hz, 1H), 7.34 (s, 1H); ¹³C NMR (100 MHz, DMSO-*d*₆) δ 165.9, 153.2, 142.3, 135.7, 130.6, 128.7, 128.2, 127.1 (q, ¹J_{CF} = 222 Hz), 126.9, 126.0–126.2 (m, two overlapping carbons), 125.8, 123.8, 122.6, 120.1, 110.5; HRESI-MS for [C₁₈H₁₂F₃NO₂-H]⁻, Calcd 330.0747. Found 330.0743.

4.1.9. 3-Hydroxy-*N*-(4-methoxyphenyl)-2-naphthamide (1j)

Amide **1j** was obtained using general procedure A as a light green solid in 45% yield: mp 218–220 °C (Lit.³⁹ 229.5–230.5 °C). ¹H NMR (400 MHz, DMSO-*d*₆) δ 11.49 (s, 1H), 10.51 (s, 1H), 8.52 (s, 1H), 7.91 (d, *J* = 7.6 Hz, 1H), 7.76 (d, *J* = 8.0 Hz, 1H), 7.66 (d, *J* = 8.8 Hz, 2H), 7.51 (t, *J* = 7.6 Hz, 1H), 7.36 (t, *J* = 8.0 Hz, 1H), 7.32 (s, 1H), 6.96 (d, *J* = 8.8 Hz, 2H), 3.76 (s, 3H); ¹³C NMR (100 MHz, DMSO-*d*₆) δ 165.6, 155.9, 154.1, 135.8, 131.3, 130.2, 128.7, 128.1, 126.8, 125.8, 123.7, 122.3, 121.1, 113.9, 110.6, 55.2; HRESI-MS for [C₁₈H₁₅NO₃-H]⁻, Calcd 292.0979. Found 292.0977.

4.1.10. *N*-(3,4-Difluorophenyl)-3-hydroxy-2-naphthamide (1k)

Amide **1k** was obtained using general procedure A as an off-white solid in 90% yield: mp 254–256 °C. ¹H NMR (400 MHz, DMSO-*d*₆) δ 11.15 (s, 1H), 10.72 (s, 1H), 8.42 (s, 1H), 7.91–8.00 (m, 2H), 7.76 (d, *J* = 8.4 Hz, 1H), 7.42–7.52 (m, 3H), 7.33–7.38 (m, 2H); ¹³C NMR (100 MHz, DMSO-*d*₆) δ 165.7, 153.3, 148.9 (dd, *J* = 242, 13 Hz), 145.7 (dd, *J* = 240, 12 Hz), 135.7–135.6 (m, 1 C), 130.4, 128.7, 128.1, 126.8, 125.8, 123.8, 122.3, 117.5 (d, *J* = 18 Hz), 116.7 (d, *J* = 6 Hz), 110.5, 109.4 (d, *J* = 22 Hz); HRESI-MS for [C₁₇H₁₁F₂NO₂-H]⁻, Calcd 298.0685. Found 298.0680.

4.1.11. *N*-(3-Chloro-4-fluorophenyl)-3-hydroxy-2-naphthamide (1l)

Amide **1l** was obtained using general procedure A as a beige solid in 73% yield: mp 250–252 °C. ¹H NMR (400 MHz, DMSO-*d*₆) δ 11.11 (s, 1H), 10.70 (s, 1H), 8.42 (s, 1H), 8.10 (dd, *J* = 6.8, 2.4 Hz, 1H), 7.93 (d, *J* = 8.0 Hz, 1H), 7.77 (d, *J* = 8.0 Hz, 1H), 7.68–7.72 (m, 1H), 7.51 (t, *J* = 7.2 Hz, 1H), 7.45 (t, *J* = 9.2 Hz, 1H), 7.36 (t, *J* = 7.2 Hz, 1H), 7.33 (s, 1H); ¹³C NMR (100 MHz, DMSO-*d*₆) δ 165.7, 153.4, 152.3, 135.9, 135.7, 130.4, 128.7, 128.2, 126.8, 125.8, 123.8, 122.3, 121.8, 120.7 (d, *J* = 7 Hz), 119.2 (d, *J* = 18 Hz), 117.0 (d, *J* = 21 Hz), 110.5; HRESI-MS for [C₁₇H₁₁ClFNO₂-H]⁻, Calcd 314.0390. Found 314.0389.

4.1.12. 2,2-Dimethyl-4*H*-naphtho[2,3-*d*][1,3]dioxin-4-one (9)

Ac₂O (1 mL) and acetone (5 mL) were sequentially added to acid **2** (1.88 g, 10 mmol) at room temperature. The resulting mixture was then cooled to -80 °C and then concentrated H₂SO₄ (0.1 mL) was added. The reaction mixture was allowed to warm up to room temperature and stirred at room temperature for 12 h. The solvents were removed under reduced pressure. Hexanes (30 mL) were added and then removed under reduced pressure. This was repeated three times to remove residual solvents from the brown solid, which was then purified by column chromatography eluting with hexanes/EtOAc (20:1) to yield a light yellow powder (215 mg, 9.4%); mp 104–106 °C. ¹H NMR (400 MHz, DMSO-*d*₆) δ 8.58 (s, 1H), 7.89 (d, *J* = 8.4 Hz, 1H), 7.44 (d, *J* = 8.0 Hz, 1H), 7.55 (td, *J* = 8.0, 1.2 Hz, 1H), 7.42 (td, *J* = 8.0, 1.2 Hz, 1H), 7.32 (s, 1H), 1.74 (s, 6H); ¹³C NMR (100 MHz, DMSO-*d*₆) δ 161.5, 151.2, 137.7, 132.2, 129.7, 129.6, 129.1, 126.9, 125.4, 114.2, 112.8, 106.3, 26.2.

4.1.13. 3-Hydroxy-*N*-(pyridin-2-yl)-2-naphthamide (10a)⁴⁰

Amide **10a** was obtained using general procedure B as an off-white solid in 87% yield: mp 254–256 °C (dec). ¹H NMR (400 MHz, DMSO-*d*₆) δ 11.71 (br s, 1H), 11.13 (s, 1H), 8.69 (s, 1H), 8.38 (dt, *J* = 4.8, 0.8 Hz, 1H), 8.33 (d, *J* = 8.4 Hz, 1H), 7.99 (d, *J* = 8.4 Hz, 1H), 7.88 (td, *J* = 8.4, 2.0 Hz, 1H), 7.79 (d, *J* = 8.4 Hz, 1H), 7.53 (t, *J* = 8.0 Hz, 1H), 7.36–7.39 (m, 2H), 7.18 (td, *J* = 6.0, 0.8 Hz, 1H); ¹³C NMR (100 MHz, DMSO-*d*₆) δ 163.8, 152.7, 151.6, 148.3, 138.5, 136.0, 132.6, 129.1, 128.5, 127.2, 125.7, 124.0, 120.9, 120.0, 114.0, 110.9; HRESI-MS for [C₁₆H₁₂N₂O₂+H]⁺, Calcd 265.0972. Found 265.0974.

4.1.14. 3-Hydroxy-*N*-(pyridin-4-yl)-2-naphthamide (10b)

Amide **10b** was obtained using slightly modified general procedure B as a yellow solid in 87% yield. Briefly, after the reaction was complete (2 h), the solvent was removed under reduced pressure to give a yellow residue that was subjected to column chromatography eluting with CH₂Cl₂-MeOH (20:1) to give **10b**: mp > 262 °C (dec). ¹H NMR (400 MHz, DMSO-*d*₆) δ 11.08 (br s, 1H), 10.84 (br s, 1H), 8.50 (d, *J* = 6.4 Hz, 2H), 8.40 (s, 1H), 7.94 (d, *J* = 8.4 Hz, 1H), 7.75–7.78 (m, 3H), 7.51 (td, *J* = 8.4, 1.2 Hz, 1H), 7.36 (td, *J* = 8.0, 1.2 Hz, 1H), 7.33 (s, 1H); ¹³C NMR (100 MHz, DMSO-*d*₆) δ 166.2, 153.0, 150.4, 145.4, 135.7, 130.7, 128.7, 128.2, 126.9, 125.8, 123.8, 122.9, 114.0, 110.4; HRESI-MS for [C₁₆H₁₂N₂O₂+H]⁺, Calcd 265.0972. Found 265.0975.

4.1.15. 3-Hydroxy-*N*-(pyrazin-2-yl)-2-naphthamide (10c)

Amide **10c** was obtained using general procedure B as an off-white solid in 76% yield: mp > 228 °C. ¹H NMR (400 MHz, DMSO-*d*₆) δ 11.75 (br s, 1H), 11.29 (br s, 1H), 9.58 (s, 1H), 8.67 (s, 1H), 8.45–8.48 (m, 2H), 7.99 (d, *J* = 8.4 Hz, 1H), 7.79 (d, *J* = 8.4 Hz, 1H), 7.54 (t, *J* = 7.6 Hz, 1H), 7.36–7.39 (m, 2H); ¹³C NMR (100 MHz, DMSO-*d*₆) δ 164.0, 152.7, 148.4, 142.9, 140.3, 136.6, 136.2, 132.6, 129.1, 128.6, 127.1, 125.8, 124.0, 120.6, 110.9; HRESI-MS for [C₁₅H₁₁N₃O₂-H]⁻, Calcd 264.0779. Found 264.0773.

4.2. Biology

4.2.1. General information

pCRE-RLuc and pVP16-CREB were described previously.¹⁷ A549 and human foreskin fibroblast (HFF) were obtained from American Tissue Culture Collection (ATCC, Manassas, VA). MCF-7, MDA-MB-231 and MDA-MB-468 cells were obtained from Development Therapeutics Program at the National Cancer Institute. The cells were maintained in Dulbecco's modified Eagle medium (DMEM, Invitrogen, Carlsbad, CA) supplemented with 10% (v/v) fetal bovine serum (FBS), 10 μg/mL penicillin and 10 μg/mL streptomycin (Invitrogen, Carlsbad, CA) at 37 °C under 5% CO₂. The primary

antibodies used were obtained from commercial sources: anti-poly (ADP-ribose) polymerase (PARP), anti-CREB, anti-Bcl-2, anti-p21 were from Cell Signaling Technology (Danvers, MA); anti-glyceraldehyde-3-phosphate dehydrogenase (GAPDH) and M2 (anti-FLAG) were from Sigma (St. Louis, MO); horseradish peroxidase (HRP)-conjugated secondary antibodies were from Bio-Rad (Hercules, CA). VEGF ELISA assay kit was from R&D Systems (Minneapolis, MN).

4.2.2. Western blot

Exponentially growing A549 cells were treated with **1a** at different concentrations for 48 h. The cells were then harvested and washed twice with cold PBS (pH 7.4). The cell pellets were then lysed in Nonidet P-40 lysis buffer (50 mM TrisHCl, pH 8.0, 5 mM EDTA, 150 mM NaCl, 1 mM DTT, 0.5% Nonidet P-40) containing 8 M urea. Then equal amount of proteins was loaded and separated on a 10% or 4–20% SDS-PAGE gel. The proteins were then transferred to a PVDF membrane (Bio-Rad, Hercules, CA) and blotted with various antibodies.

4.2.3. Flow cytometry

Exponentially growing A549 cells were treated with different concentrations of **1a** for 48 h. The cells were then harvested and washed twice with cold PBS (pH 7.4). Flow cytometric analysis was carried out with Annexin V-FITC Apoptosis Detection Kit I (BD Biosciences, Franklin Lakes, NJ) and BD FACS Calibur following manufacturer's instructions.

4.2.4. Inhibition of CREB-mediated gene transcription

HEK 293T cells in a 10-cm plate were transfected with pCRE-RLuc (6.0 μ g) using Lipofectamine™ 2000 (Invitrogen, Carlsbad, CA) according to manufacturer's protocol. After 3 h, the transfected cells were collected and replated into 96-well plates (1–2 \times 10⁴ cells/well). The cells were allowed to attach to the bottom of the wells for overnight, when compounds of different concentrations were added to the cells. Forskolin (final concentration of 10 μ M, LC Laboratories, Woburn, MA) was added 30 min after the addition of the compounds. The cells were then incubated at 37 °C for 5 h. The media in the wells were removed and the cells were then lysed in 30 μ L of 1X Renilla luciferase lysis buffer (Promega, Madison, WI). To measure Renilla luciferase activity, 5 μ L of the lysate was combined with 30 μ L of benzyl-coelenterazine (Nanolight, Pinetop, AZ) solution in PBS (pH 7.4, 10 μ g/mL). The sample protein concentration was determined by Dye Reagent Concentrate (Bio-Rad, Hercules, CA). The Renilla luciferase activity was normalized to protein content in each well and expressed as relative luciferase unit/ μ g protein (RLU/ μ g protein). The IC₅₀ was derived from non-linear regression analysis of the RLU/ μ g protein-concentration curve in Prism 5.0 (La Jolla, CA).

4.2.5. Quantitative RT-PCR

Exponentially growing A549 cells were treated with compound **1a** for 4 h and then total RNA was extracted using RNeasy (QIAGEN, Valencia, CA). Total RNA was then treated with TURBO DNA-free™ (Ambion, Austin, TX) at 37 °C for 30 min to remove genomic DNA contamination. The cDNA was synthesized using SuperScript III First-Strand Synthesis System for RT-PCR (Invitrogen, Carlsbad, CA) and random primers according to the manufacturer's instructions. Quantitative PCR was performed with ABI 7500 Fast System using SYBR® Advantage® qPCR Pre-mix (Clontech, Mountain View, CA). Hypoxanthine phosphoribosyltransferase (HPRT) was employed as the reference gene to normalize input amounts and to perform relative quantifications by the 2^{- $\Delta\Delta$ Ct} method.^{41,42} Primer sequences are available upon request.

4.2.6. In vitro KIX–KID Renilla luciferase complementation assay

RLuc-KIX (20 ng/reaction) and KID-RLuc-containing cell lysates (1.0 μ g/reaction), both of which were prepared as described before,¹⁷ were mixed together in 1X Renilla luciferase lysis buffer in the presence of different concentrations of different compounds. The final volume of the incubation mixture was 40 μ L. The mixture was incubated at 4 °C for 20–24 h. Then residual Renilla luciferase activity was measured by combining 5 μ L of the incubation mixture with 30 μ L of benzyl-coelenterazine solution in PBS (pH 7.4, 10 μ g/mL) and expressed as RLU. The IC₅₀ was derived from non-linear regression analysis of the RLU-concentration curve in Prism 5.0.

4.2.7. Establishment of MCF-7 cells expressing VP16-CREB and MTT Assay

MCF-7 cells were transfected with a plasmid encoding Flag-tagged VP16-CREB¹⁷ by Lipofectamine™ 2000 according to manufacturer's protocol. Two days after transfection, the media were changed to selection media containing 2 mg/mL of G418 (Invitrogen, Carlsbad, CA) until a stable colony was formed. The growth inhibition was assessed by 3-(4,5-dimethyl-2-thiazolyl)-2,5-diphenyl-2H-tetrazolium bromide (MTT reagent, Sigma, St. Louis, MO) assay as described.^{22,43} Percent of growth is defined as $100\% \times (A_{\text{treated}} - A_{\text{initial}}) / (A_{\text{control}} - A_{\text{initial}})$, where A_{treated} represents absorbance at 570 nm in wells treated with a compound, A_{initial} represents the absorbance at time 0 and A_{control} denotes media-treated cells. The GI₅₀ was derived from non-linear regression analysis of the percent of growth-concentration curve in Prism 5.0.

4.2.8. HMEC and HFF growth inhibition

Human mammary epithelial cells (HMEC, Lonza, Walkersville, MA) were routinely cultured in MEGM complete media (Lonza) supplemented with 10 μ g/mL penicillin and 10 μ g/mL streptomycin (Invitrogen, Carlsbad, CA) at 37 °C under 5% CO₂. On the day of treatment with compound **1a** in 6-well plates, the media were changed to DMEM supplemented with 10% FBS, 10 μ g/mL penicillin and 10 μ g/mL streptomycin. Then various concentrations of compound **1a** were added and the cells were incubated with the compound for 48 h. The number of live cells was then determined by trypan blue exclusion assay.

4.2.9. Statistical analysis

The data are expressed as mean \pm SD. One-way analysis of variance (ANOVA, Prism) or paired two-tailed *t*-test (Microsoft Excel) was used to assess the statistical differences. A *P* value of less than 0.05 was considered significant.

Acknowledgments

We thank Drs. Grover Bagby and Richard Goodman for helpful comments and discussions, and Dr. Rosalie Sears for a critical reading of the manuscript. We thank Ms. Pamela Canaday and Martha Bosch for technical assistance with flow cytometry and qPCR, respectively. Developmental Therapeutics Program at NCI is appreciated for evaluating growth inhibitory activity of **1a** in NCI's panel of cancer cell lines. This work was made possible by financial supports from Susan G. Komen for the Cure (KG100458) and NIH (R01GM087305). We thank Dr. Andrea DeBarber for running the mass spectroscopic analyses.

Supplementary data

Supplementary data associated with this article can be found, in the online version, at <http://dx.doi.org/10.1016/j.bmc.2012.09.056>.

These data include MOL files and InChIKeys of the most important compounds described in this article.

References

1. Darnell, J. E., Jr. *Nat. Rev. Cancer* **2002**, *2*, 740.
2. Xiao, X.; Li, B. X.; Mitton, B.; Ikeda, A.; Sakamoto, K. M. *Curr. Cancer Drug Targets* **2010**, *10*, 384.
3. Sakamoto, K. M.; Frank, D. A. *Clin. Cancer Res.* **2009**, *15*, 2583.
4. Shaywitz, A. J.; Greenberg, M. E. *Annu. Rev. Biochem.* **1999**, *68*, 821.
5. Johannessen, M.; Moens, U. In *Trends in Cellular Signaling*; Caplin, D. E., Ed.; Nova Publishers, 2006; p 41.
6. Radhakrishnan, I.; PerezAlvarado, G. C.; Parker, D.; Dyson, H. J.; Montminy, M. R.; Wright, P. E. *Cell* **1997**, *91*, 741.
7. Conkright, M. D.; Montminy, M. *Trends Cell Biol.* **2005**, *15*, 457.
8. Wu, W.; Zhau, H. E.; Huang, W. C.; Iqbal, S.; Habib, F. K.; Sartor, O.; Cvitanovic, L.; Marshall, F. F.; Xu, Z.; Chung, L. W. K. *Oncogene* **2007**, *26*, 5070.
9. Chhabra, A.; Fernando, H.; Watkins, G.; Mansel, R. E.; Jiang, W. G. *Oncol. Rep.* **2007**, *18*, 953.
10. Seo, H. S.; Liu, D. D.; Bekele, B. N.; Kim, M. K.; Pisters, K.; Lippman, S. M.; Wistuba, II; Koo, J. S. *Cancer Res.* **2008**, *68*, 6065.
11. Shankar, D. B.; Cheng, J. C.; Kinjo, K.; Federman, N.; Moore, T. B.; Gill, A.; Rao, N. P.; Landaw, E. M.; Sakamoto, K. M. *Cancer Cell* **2005**, *7*, 351.
12. Pigazzi, M.; Manara, E.; Baron, E.; Basso, G. *Cancer Res.* **2009**, *69*, 2471.
13. Crans-Vargas, H. N.; Landaw, E. M.; Bhatia, S.; Sandusky, G.; Moore, T. B.; Sakamoto, K. M. *Blood* **2002**, *99*, 2617.
14. Park, Y. G.; Nesterova, M.; Agrawal, S.; Cho-Chung, Y. S. *J. Biol. Chem.* **1999**, *274*, 1573.
15. Xie, S. H.; Price, J. E.; Luca, M.; Jean, D.; Ronai, Z.; Bar-Eli, M. *Oncogene* **1997**, *15*, 2069.
16. Abramovitch, R.; Tavor, E.; Jacob-Hirsch, J.; Zeira, E.; Amariglio, N.; Pappo, O.; Rechavi, G.; Galun, E.; Honigman, A. *Cancer Res.* **2004**, *64*, 1338.
17. Li, B. X.; Xiao, X. *ChemBioChem* **2009**, *10*, 2721.
18. Liechti, C.; Sequin, U.; Bold, G.; Furet, P.; Meyer, T.; Traxler, P. *Eur. J. Med. Chem.* **2004**, *39*, 11.
19. Kang, S. W.; Gothard, C. M.; Maitra, S.; Atia Tul, W.; Nowick, J. S. *J. Am. Chem. Soc.* **2007**, *129*, 1486.
20. Jiang, M.; Li, B. X.; Xie, F.; Delaney, F.; Xiao, X. *J. Med. Chem.* **2012**, *55*, 4020.
21. Chen, I. J.; Taneja, R.; Yin, D.; Seo, P. R.; Young, D.; MacKerell, A. D., Jr.; Polli, J. E. *Mol. Pharm.* **2006**, *3*, 745.
22. Mosmann, T. J. *Immunol. Methods* **1983**, *65*, 55.
23. Zhang, X. M.; Odom, D. T.; Koo, S. H.; Conkright, M. D.; Canettieri, G.; Best, J.; Chen, H. M.; Jenner, R.; Herbolsheimer, E.; Jacobsen, E.; Kadam, S.; Ecker, J. R.; Emerson, B.; Hogenesch, J. B.; Unterman, T.; Young, R. A.; Montminy, M. *Proc. Natl. Acad. Sci. U.S.A.* **2005**, *102*, 4459.
24. Belkhiri, A.; Dar, A. A.; Zaika, A.; Kelley, M.; El-Rifai, W. *Cancer Res.* **2008**, *68*, 395.
25. Wilson, B. E.; Mochon, E.; Boxer, L. M. *Mol. Cell. Biol.* **1996**, *16*, 5546.
26. Cory, S.; Adams, J. M. *Nat. Rev. Cancer* **2002**, *2*, 647.
27. Abou El Hassan, M. A.; Mastenbroek, D. C.; Gerritsen, W. R.; Giaccone, G.; Kruyt, F. A. *Br. J. Cancer* **2004**, *91*, 171.
28. Eldeiry, W. S.; Tokino, T.; Velculescu, V. E.; Levy, D. B.; Parsons, R.; Trent, J. M.; Lin, D.; Mercer, W. E.; Kinzler, K. W.; Vogelstein, B. *Cell* **1993**, *75*, 817.
29. Best, J. L.; Amezcua, C. A.; Mayr, B.; Flechner, L.; Murawsky, C. M.; Emerson, B.; Zor, T.; Gardner, K. H.; Montminy, M. *Proc. Natl. Acad. Sci. U.S.A.* **2004**, *101*, 17622.
30. Balasubramanian, K.; Schroit, A. J. *Annu. Rev. Physiol.* **2003**, *65*, 701.
31. Vermes, I.; Haanen, C.; Steffensnakken, H.; Reutelingsperger, C. J. *Immunol. Methods* **1995**, *184*, 39.
32. Tewari, M.; Quan, L. T.; Orourke, K.; Desnoyers, S.; Zeng, Z.; Beidler, D. R.; Poirier, G. G.; Salvesen, G. S.; Dixit, V. M. *Cell* **1995**, *81*, 801.
33. Tao, X.; Finkbeiner, S.; Arnold, D. B.; Shaywitz, A. J.; Greenberg, M. E. *Neuron* **1998**, *20*, 709.
34. Evan, G. I.; Wyllie, A. H.; Gilbert, C. S.; Littlewood, T. D.; Land, H.; Brooks, M.; Waters, C. M.; Penn, L. Z.; Hancock, D. C. *Cell* **1992**, *69*, 119.
35. Mayr, B.; Montminy, M. *Nat. Rev. Mol. Cell Biol.* **2001**, *2*, 599.
36. Hummler, E.; Cole, T. J.; Blendy, J. A.; Ganss, R.; Aguzzi, A.; Schmid, W.; Beerermann, F.; Schutz, G. *Proc. Natl. Acad. Sci. U.S.A.* **1994**, *91*, 5647.
37. Tripathy, H.; Pradhan, D. G.; Dash, B. C.; Mahapatra, G. N. *Agric. Biol. Chem.* **1973**, *37*, 1375.
38. Knaggs, S.; Malkin, H.; Osborn, H. M. I.; Williams, N. A. O.; Yaqoob, P. *Org. Biomol. Chem.* **2005**, *3*, 4002.
39. Schnopper, I.; Broussard, J. O.; LaForgia, C. K. *Anal. Chem.* **1959**, *31*, 1542.
40. Vaillancourt, V. A.; Cudahy, M. M.; Staley, S. A.; Brideau, R. J.; Conrad, S. J.; Knechtel, M. L.; Oien, N. L.; Wieber, J. L.; Yagi, Y.; Wathen, M. W. *Bioorg. Med. Chem. Lett.* **2000**, *10*, 2079.
41. Pfaffl, M. W. *Nucleic Acids Res.* **2001**, *29*, e45.
42. Livak, K. J.; Schmittgen, T. D. *Methods* **2001**, *25*, 402.
43. Rubinstein, L. V.; Shoemaker, R. H.; Paull, K. D.; Simon, R. M.; Tosini, S.; Skehan, P.; Scudiero, D. A.; Monks, A.; Boyd, M. R. *J. Natl. Cancer Inst.* **1990**, *82*, 1113.